J|A|C|S
ARTICLES
Published on Web 01/17/2003

Proton-Coupled O−O Activation on a Redox Platform Bearing a Hydrogen-Bonding Scaffold

Christopher J. Chang, Leng Leng Chng, and Daniel G. Nocera*

Contribution from the Department of Chemistry, 6-335, Massachusetts Institute of Technology, 77 Massachusetts Avenue, Cambridge, Massachusetts 02139-4307

Received September 14, 2002; E-mail: nocera@mit.edu

Abstract: Porphyrin architectures bearing a hydrogen-bonding scaffold have been synthesized. The H-bond pendant allows proton-coupled electron transfer (PCET) to be utilized as a vehicle for effecting catalytic O−O bond activation chemistry. Suzuki cross-coupling reactions provide a modular synthetic strategy for the attachment of porphyrins to a rigid xanthene or dibenzofuran pillar bearing the H-bond pendant. The resulting HPX (hanging porphyrin xanthene) and HPD (hanging porphyrin dibenzofuran) systems permit both the orientation and acid−base properties of the hanging H-bonding group to be controlled. Comparative reactivity studies for the catalase-like disproportionation of hydrogen peroxide and the epoxidation of olefins by the HPX and HPD platforms with acid and ester hanging groups reveal that the introduction of a proton-transfer network, properly oriented to a redox-active platform, can orchestrate catalytic O−O bond activation. For the catalase and epoxidation reaction types, a marked reactivity enhancement is observed for the xanthene-bridged platform appended with a pendant carboxylic acid group, establishing that this approach can yield superior catalysts to analogues that do not control both proton and electron inventories.

Introduction

Many fundamental small-molecule transformations in nature require the coupled transport of both proton *and* electron equivalents to effect bond-making and bond-breaking catalysis. Consummate examples include the photoinduced oxidation of water to oxygen by photosystem II[1−5] and the chemically diametric reduction of oxygen to water by cytochrome *c* oxidase.[6−14] In addition to these enzymes, proton-coupled electron transfer (PCET) events continue to emerge in the structure/function relations of a broad range of other natural systems such as copper-based oxidases,[15−17] flavin- and pyrroloquinoline-dependent enzymes,[18,19] non-heme iron proteins,[20−29] and reductases such as hydrogenase[30−33] and nitrogenase,[34,35] to name a few.

Within the interiors of the complex tertiary structures of these oxidases and reductases, noncovalent hydrogen-bonding interactions are paramount to dynamically regulating the active site for PCET reactivity. Heme-dependent proteins featuring a conserved iron protoporphyrin IX cofactor are exemplary in their structural control of PCET. Figure 1 compares the active-site structures of peroxidases, catalases, and the cytochrome P450 monooxygenases, highlighting the structural parallels at the distal side of the heme pocket where O−O activation occurs. Through the targeted use of amino acid side chains and/or solvent water as proton shuttles, these proteins react with oxygen or hydrogen peroxide to generate highly reactive iron-oxo species within their active-site cavities. Such hydrogen-bonding groups participate in directed acid−base chemistry to provide

(1) Tommos, C.; Babcock, G. T. *Acc. Chem. Res.* **1998**, *31*, 18−25.
(2) Yachandra, V. K.; Sauer, K.; Klein, M. P. *Chem. Rev.* **1996**, *96*, 2927−2950.
(3) Dismukes, G. C. *Science* **2001**, *292*, 447−448.
(4) Vrettos, J. S.; Limburg, J.; Brudvig, G. W. *Biochim. Biophys. Acta* **2001**, *1503*, 229−245.
(5) Yocum, C. F.; Pecoraro, V. L. *Curr. Opin. Chem. Biol.* **1999**, *3*, 182−187.
(6) Babcock, G. T.; Wikström, M. *Nature* **1992**, *356*, 301−309.
(7) Ferguson-Miller, S.; Babcock, G. T. *Chem. Rev.* **1996**, *96*, 2889−2907.
(8) Michel, H.; Behr, J.; Harrenga, A.; Kannt, A. *Annu. Rev. Biophys. Biomol. Struct.* **1998**, *27*, 329−356.
(9) Schultz, B. E.; Chan, S. I. *Annu. Rev. Biophys. Biomol. Struct.* **2001**, *30*, 23−65.
(10) Malmström, B. G. In *Electron Transfer in Chemistry*; Balzani, V., Ed.; Wiley-VCH: Weinheim, Germany, 2001; Vol. 3.1.3, pp 39−55.
(11) Wikström, M. *Biochim. Biophys. Acta* **2000**, *1458*, 188−198.
(12) Gennis, R. B. *Proc. Natl. Acad. Sci U.S.A.* **1998**, *95*, 12747−12749.
(13) Brzezinski, P. *Biochim. Biophys. Acta* **2000**, *1458*, 1−5.
(14) Ramirez, B. E.; Malmström, B. G.; Winkler, J. R.; Gray, H. B. *Proc. Natl. Acad. Sci. U.S.A.* **1995**, *92*, 11949−11951.
(15) Klinman, J. P. *Chem. Rev.* **1996**, *96*, 2541−2561.
(16) Whittaker, M. M.; Whittaker, J. W. *Biochemistry* **2001**, *40*, 7140−7148.
(17) Solomon, E. I.; Chen, P.; Metz, M.; Lee, S.-K.; Palmer, A. E. *Angew. Chem., Int. Ed.* **2001**, *40*, 4570−4590.
(18) Silverman, R. B. *Acc. Chem. Res.* **1995**, *28*, 335−342.
(19) Davidson, V. L. *Adv. Protein Chem.* **2001**, *58*, 95−140.
(20) Guallar, V.; Gherman, B. F.; Lippard, S. J.; Friesner, R. A. *Curr. Opin. Chem. Biol.* **2002**, *6*, 236−242.
(21) Lee, S.-K.; Lipscomb, J. D. *Biochemistry* **1999**, *38*, 4423−4432.
(22) Solomon, E. I. *Inorg. Chem.* **2001**, *40*, 3656−3669.
(23) Que, L., Jr.; Ho, R. Y. N. *Chem. Rev.* **1996**, *96*, 2607−2624.
(24) Knapp, M. J.; Rickert, K.; Klinman, J. P. *J. Am. Chem. Soc.* **2002**, *124*, 3865−3874.
(25) Chen, K.; Hirst, J.; Camba, R.; Bonagura, C. A.; Stout, C. D.; Burgess, B. K.; Armstrong, F. A. *Nature* **2000**, *405*, 814−817.
(26) Armstrong, F. A. *J. Chem. Soc., Dalton Trans.* **2002**, 661−671.
(27) Chen, K.; Hirst, J.; Camba, R.; Bonagura, C. A.; Stout, C. D.; Burgess, B. K.; Armstrong, F. A. *Nature* **2000**, *405*, 814−817.
(28) Low, D. W.; Hill, M. G. *J. Am. Chem. Soc.* **2000**, *122*, 11039−11040.
(29) Kennedy, M. L.; Gibney, B. R. *J. Am. Chem. Soc.* **2002**, *124*, 6826−6827.
(30) Peters, J. W. *Curr. Opin. Struct. Biol.* **1999**, *9*, 670−676.
(31) Berkessel, A. *Curr. Opin. Chem. Biol.* **2001**, *5*, 486-490.
(32) Thauer, R. K.; Klein, A. R.; Hartmann, G. C. *Chem. Rev.* **1996**, *96*, 3031−3042.
(33) Adams, M. W. W.; Stiefel, E. I. *Curr. Opin. Chem. Biol.* **2000**, *4*, 214−220.
(34) Burgess, B. K.; Lowe, D. J. *Chem. Rev.* **1996**, *96*, 2983−3011.
(35) Rees, D. C.; Howard, J. B. *Curr. Opin. Chem. Biol.* **2000**, *4*, 559−566.

10.1021/ja028548o CCC: $25.00

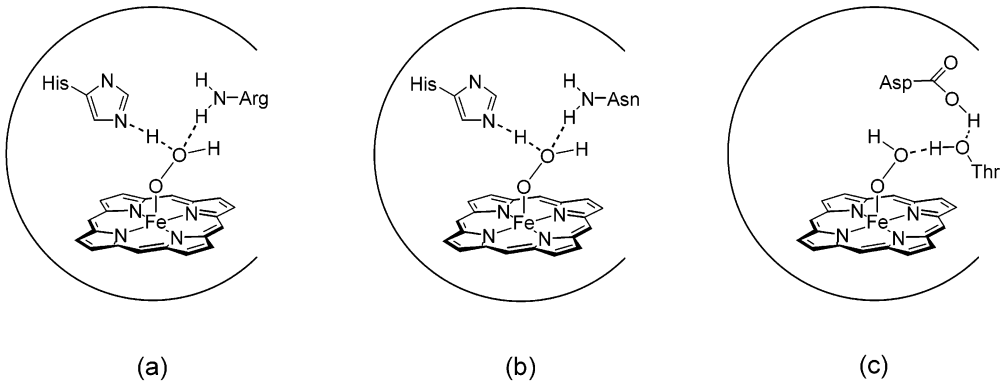

Figure 1. Comparison of proposed proton-activated O−O bond cleavage for iron-oxo heme formation in (a) peroxidases, (b) catalases, and (c) cytochrome P450 monooxygenases.

kinetic control of proton transfer and bond polarization for heterolytic O−O bond cleavage, classically known as the "pull effect".[36−40] The cytochrome P450 family of enzymes are particularly intriguing in their use of internal solvent water channels embedded within the protein superstructure to tune heme electronic structure and redox potential, as well as furnishing a possible proton-relay pathway during catalytic turnover.[41−43] With regard to this latter issue, studies with the native P450cam enzyme and its site-directed mutants[42,44−50] suggest that active-site amino acid residues (Asp and Thr) are important in establishing a controlled proton delivery pathway involving solvent water, as well as providing an active-site hydrogen-bond donor to stabilize the oxygen adduct.[51−57] From the singular point of a iron protoporphyrin IX cofactor, hemoproteins have evolved their protein structure to accommodate diverse functions,[58] including O_2 transport and storage,[59,60] single outer-sphere electron transfer,[61−63] O_2 reduction,[6−14] small-molecule sensing and signaling,[64−66] and metabolic oxidation reactions.[36,37,67] In all cases, the specific chemical reactivity of the heme enzyme is dictated by the surrounding polypeptide medium, which encapsulates the redox cofactor within a precise microenvironment for proper delivery of proton and electron equivalents.

Although the importance of hydrogen-bonding and water channels is clearly recognized in the structural biology of heme proteins, neither the origin of protons in the hydrophobic binding pockets of hemes nor the mechanism of coupled electron and proton transfer has been definitively established. To this end, several protein- and peptide-based constructs have recently been designed to probe how oxidative reactivity mediated by proton- and electron-transfer events is controlled by the heme's distal superstructure. Myoglobin has been converted into a peroxidase-like enzyme by alteration of the heme distal pocket via site-directed mutagenesis.[38] In a separate strategy, substrates tethered to photoexcitable redox triggers have been employed to scrutinize reactive transient species of cytochrome P450.[68−70] In this same vein, semisynthetic approaches have been utilized to prepare myoglobins with functionalized hemes for generating high-valent ferryl species upon photon absorption.[71,72] Combined with studies of the natural enzymes, these biomolecule-based constructs have sought to exploit the native protein fold to impose the H-bond network required for PCET activation of the O−O bond affixed to the heme active site.

Owing to the challenges associated with isolating and identifying the precise factors governing PCET in complex

(36) Sono, M.; Roach, M. P.; Coulter, E. D.; Dawson, J. H. *Chem. Rev.* **1996**, *96*, 2841−2887.
(37) Ortiz de Montellano, P. R. *Cytochrome P450: Structure, Mechanism, and Biochemistry*, 2nd ed.; Plenum: New York, 1995.
(38) Ozaki, S.-I.; Roach, M. P.; Matsui, T.; Watanbe, Y. *Acc. Chem. Res.* **2001**, *34*, 818−825.
(39) Everse, J.; Everse, K. E.; Grisham, M. B. *Peroxidases in Chemistry and Biology*; CRC Press: Boca Raton, FL, 1991; Vol. I and II.
(40) Dawson, J. H. *Science* **1988**, *240*, 433−439.
(41) Oprea, T. I.; Hummer, G.; García, A. E. *Proc. Natl. Acad. Sci. U.S.A.* **1997**, *94*, 2133−2138.
(42) Vidakovic, M.; Sligar, S. G.; Li, H.; Poulos, T. L. *Biochemistry* **1998**, *37*, 9211−9219.
(43) Poulos, T. L. *Curr. Opin. Struct. Biol.* **1995**, *5*, 767−774.
(44) Imai, M.; Shimada, H.; Watanbe, Y.; Matsushima-Hubiya, Y.; Makino, R.; Koga, H.; Horiuchi, R.; Ishimura, Y. *Proc. Natl. Acad. Sci. U.S.A.* **1989**, *86*, 7823−7827.
(45) Martinis, S. A.; Atkins, W. M.; Stayton, P. S.; Sligar, S. G. *J. Am. Chem. Soc.* **1989**, *111*, 9252−9253.
(46) Gerber, N. C.; Sligar, S. G. *J. Am. Chem. Soc.* **1992**, *114*, 8742−8743.
(47) Benson, D. E.; Suslick, K. S.; Sligar, S. G. *Biochemistry* **1997**, *36*, 5104−5107.
(48) Hasemann, C. A.; Kurumbail, R. G.; Boddupalli, S. S.; Peterson, J. A.; Deisenhofer, J. *Structure* **1995**, *3*, 41−62.
(49) Poulos, T. L.; Raag, R. *FASEB J.* **1991**, *6*, 674−679.
(50) Newcomb, N.; Shen, R.; Choi, S.-Y.; Toy, P. H.; Hollenberg, P. F.; Vaz, A. D. N.; Coon, M. J. *J. Am. Chem. Soc.* **2000**, *122*, 2677−2686.
(51) Schlichting, I.; Berendzen, J.; Chu, K.; Stock, A. M.; Maves, S. A.; Benson, D. E.; Sweet, R. M.; Ringe, D.; Petsko, G. A.; Sligar, S. G. *Science* **2000**, *287*, 1615−1622.
(52) Gerber, N. C.; Sligar, S. G. *J. Biol. Chem.* **1994**, *269*, 4260−4266.
(53) Cupp-Vickery, J. R.; Poulos, T. L. *Nat. Struct. Biol.* **1995**, *2*, 144−153.
(54) Deng, T.-j.; Macdonald, I. D. G.; Simianu, M. C.; Sykora, M.; Kincaid, J. R.; Sligar, S. G. *J. Am. Chem. Soc.* **2001**, *123*, 269−278.
(55) Aikens, J.; Sligar, S. G. *J. Am. Chem. Soc.* **1994**, *116*, 1143−1144.
(56) Guallar, V.; Harris, D. L.; Batistia, V. S.; Miller, W. H. *J. Am. Chem. Soc.* **2002**, *124*, 1430−1437.
(57) Davydov, R.; Makris, T. M.; Kofman, V.; Werst, D. E.; Sligar, S. G.; Hoffman, B. M. *J. Am. Chem. Soc.* **2001**, *123*, 1403−1415.
(58) Chapman, S. K.; Daff, S.; Munro, A. W. *Struct. Bonding* **1997**, *88*, 39−70.
(59) Perutz, M. F. *Nature* **1970**, *228*, 726−734.
(60) Dickerson, R. E.; Geis, I. *Hemoglobin: Structure, Function, Evolution, and Pathology*; Benjamin/Cummings: Menlo Park, CA, 1983.
(61) Scott, R. A.; Mauk, A. G. *Cytochrome c: A Multidisciplinary Approach*; University Science Books: Sausalito, CA, 1996.
(62) Stellwagen, E. *Nature* **1978**, *275*, 73−74.
(63) Gray, H. B.; Winkler, J. R. In *Electron Transfer in Chemistry*; Balzani, V., Ed.; Wiley-VCH: Weinheim, Germany, 2001; Vol. 3.1.1, pp 3−23.
(64) Marletta, M. A.; Hurshman, A. R.; Rusche, K. M. *Curr. Opin. Chem. Biol.* **1998**, *2*, 656−663.
(65) Wasser, I. M.; de Vries, S.; Moeenne-Loccoz, P.; Schroeder, I.; Karlin, K. D. *Chem. Rev.* **2002**, *102*, 1201−1234.
(66) Chan, M. K. *Curr. Opin. Chem. Biol.* **2001**, *5*, 216−222.
(67) Groves, J. T.; Han, Y. In *Cytochrome P450: Structure, Mechanism, and Biochemistry*, 2nd ed.; Ortiz de Montellano, P. R., Ed.; Plenum: New York, 1995; pp 3−48.
(68) Dunn, A. R.; Dmochowski, I. J.; Bilwes, A. M.; Gray, H. B.; Crane, B. R. *Proc. Natl. Acad. Sci. U.S.A.* **2001**, *98*, 12420−12425.
(69) Dmochowski, I. J.; Crane, B. R.; Wilker, J. J.; Winkler, J. R.; Gray, H. B. *Proc. Natl. Acad. Sci. U.S.A.* **1999**, *96*, 12987−12990.
(70) Wilker, J. J.; Dmochowski, I. J.; Dawson, J. H.; Winkler, J. R.; Gray, H. B. *Angew. Chem., Int. Ed.* **1999**, *38*, 90−92.
(71) Hamachi, I.; Tsukiji, S.; Shinkai, S.; Oishi, S. *J. Am. Chem. Soc.* **1999**, *121*, 5500−5506.
(72) Hu, Y.-Z.; Tsukiji, S.; Shinkai, S.; Oishi, S.; Hamachi, I. *J. Am. Chem. Soc.* **2000**, *122*, 241−253.

bioconjugates, we have taken the alternative approach of molecular design by chemical synthesis. We have sought to combine acid−base and redox functionalities onto a single molecular platform. Such simple constructs, in principle, allow for the systematic control of structural and electronic variables through targeted synthetic modification. Initial efforts have explored the assembly of donor−acceptor redox pairs via hydrogen-bonding interfaces,[73−75] such as that afforded from the association of an amidinium and carboxylate.[76−81] This salt-bridge interface combines the dipole of an electrostatic ion-pair interaction with a hydrogen-bonding scaffold, allowing us to investigate how proton motion within a hydrogen-bonded interface affects the charge, energetics, and polarity of the electron transport chain.

Whereas such systems have been invaluable in elucidating mechanistic details of PCET, they are not suitable scaffolds for exploring PCET as it pertains to small-molecule activation chemistry. Proximate acid−base and redox sites are presented in a side-to-side arrangement, thus orienting the PCET functionalities orthogonal to the catalytic bond-making and bond-breaking processes required to occur at the metal center. To direct PCET toward the metal coordination site of catalytic small-molecule activation, we sought to create constructs where proton and electron delivery are confined to a face-to-face arrangement.

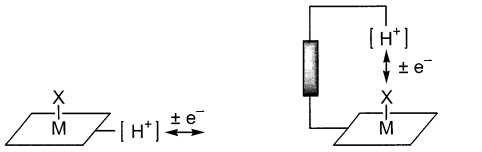

side-to-side PCET networks face-to-face PCET networks

Along these lines, we have recently demonstrated that xanthene and dibenzofuran spacers can organize two redox cofactors along the desired face-to-face reaction coordinate.[82−87] In these DPX (diporphyrin xanthene) and DPD (diporphyrin dibenzofuran) cofacial constructs, neighboring porphyrins display an extensive range of vertical pocket size dimensions and flexibilities with minimal lateral displacements between macrocyclic subunits. Replacement of one of the porphyrin redox subunits with a proton donor converts these cofacial Pacman systems into hybrid proton/redox shuttle platforms. We have recently shown that a xanthene anchor may be used to "hang" a hydrogen-bond functionality over a redox-active metalloporphyrin platform.[88,89] These Hangman architectures are simplified constructs of biomolecules with engineered distal sites inasmuch as the platforms capture control of both the proton and electron transfer but without the need for secondary and tertiary protein structure to impose a proton network among structured water or protonated amino acid side chains.

In this report, we describe the synthesis, characterization, and catalytic O−O bond activation chemistry of Hangman porphyrin platforms. Suzuki cross-coupling methods provide a smooth synthetic inroad toward the preparation of Hangman systems based on xanthene (HPX = hanging porphyrin xanthene) and dibenzofuran (HPD = hanging porphyrin dibenzofuran) scaffolds. These simple constructs allow for precise control over the functional nature of the hydrogen-bonding group in terms of proton-donating ability and arrangement in relation to the metalloporphyrin redox site. We have evaluated the catalytic O−O bond activation reactivity of a systematic set of HPX and HPD compounds with varying hydrogen-bonding and proton-transfer abilities. Two catalytic reactivities, catalase-like oxygen evolution and cytochrome P450-type epoxidation, of simple redox-only porphyrin analogues with similar steric and electronic properties have been compared to the Hangman templates. Our findings reveal that catalytic oxidation reactivity can be dramatically enhanced with a single well-positioned acid−base functionality and engender divergent chemical reactivity for a single redox cofactor.

Results

Hangman Porphyrins Bridged by Xanthene (HPX) and Dibenzofuran (HPD). An approach akin to that used for the assembly of cofacial DPX and DPD Pacman porphyrins may be employed to create asymmetric cofacial porphyrin architectures that are the subject of this report. A rigid xanthene or dibenzofuran scaffold provides the anchor point on which to affix a hydrogen-bonding group above the metal center of a porphyrin motif (HPX = hanging porphyrin xanthene, HPD = hanging porphyrin dibenzofuran). As observed for the cofacial Pacman constructs, substitution of the six-membered center ring of xanthene with the five-membered one of dibenzofuran allows for a large span of vertical distances between ditopic sites.[85] The HPX and HPD complexes are delivered according to the methods outlined in Scheme 1. We have exploited the finesse of metal-catalyzed Suzuki cross-coupling reactions to afford a facile and modular synthetic entry toward the preparation of these cofacial platforms. Notably, the Suzuki routes augment the Lindsey-type syntheses that have been previously used to produce a library of porphyrin architectures bearing functionalized xanthene spacers.[88]

The appropriate xanthene and dibenzofuran bridge precursors are readily available from dihalide starting materials. Regioselective monolithiation of Rebek's xanthene dibromide **1** with

(73) Chang, C. J.; Brown, J. D. K.; Chang, M. C. Y.; Baker, E. A.; Nocera, D. G. In *Electron Transfer in Chemistry*; Balzani, V., Ed.; Wiley-VCH: Weinheim, Germany, 2001; Vol. 3.2.4, pp 409−461.
(74) Cukier, R. I.; Nocera, D. G. *Annu. Rev. Phys. Chem.* **1998**, *49*, 337−369.
(75) Turró, C.; Chang, C. K.; Leroi, G. E.; Cukier, R. I.; Nocera, D. G. *J. Am. Chem. Soc.* **1992**, *114*, 4013−4015.
(76) Yeh, C.-Y.; Miller, S. E.; Carpenter, S. D.; Nocera, D. G. *Inorg. Chem.* **2001**, *40*, 3643−3646.
(77) Kirby, J. P.; Roberts, J. A.; Nocera, D. G. *J. Am. Chem. Soc.* **1997**, *119*, 9230−9236.
(78) Roberts, J. A.; Kirby, J. P.; Wall, S. T.; Nocera, D. G. *Inorg. Chim. Acta* **1997**, *263*, 395−405.
(79) Deng, Y.; Roberts, J. A.; Peng, S.-M.; Chang, C. K.; Nocera, D. G. *Angew. Chem., Int. Ed. Engl.* **1997**, *36*, 2124−2127.
(80) Kirby, J. P.; van Dantzig, N. A.; Chang, C. K.; Nocera, D. G. *Tetrahedron Lett.* **1995**, *36*, 3477−3480.
(81) Roberts, J. A.; Kirby, J. P.; Nocera, D. G. *J. Am. Chem. Soc.* **1995**, *117*, 8051−8052.
(82) Chang, C. J.; Deng, Y.; Heyduk, A. F.; Chang, C. K.; Nocera, D. G. *Inorg. Chem.* **2000**, *39*, 959−966.
(83) Deng, Y.; Chang, C. J.; Nocera, D. G. *J. Am. Chem. Soc.* **2000**, *122*, 410−411.
(84) Chang, C. J.; Deng, Y.; Shi, C.; Chang, C. K.; Anson, F. C.; Nocera, D. G. *Chem. Commun.* **2000**, 1355−1356.
(85) Chang, C. J.; Baker, E. A.; Pistorio, B. J.; Deng, Y.; Loh, Z.-H.; Miller, S. E.; Carpenter, S. D.; Nocera, D. G. *Inorg. Chem.* **2002**, *41*, 3102−3109.
(86) Chang, C. J.; Deng, Y.; Lee, G.-H.; Peng, S.-M.; Yeh, C.-Y.; Nocera, D. G. *Inorg. Chem.* **2002**, *41*, 3008−3016.
(87) Pistorio, B. J.; Chang, C. J.; Nocera, D. G. *J. Am. Chem. Soc.* **2002**, *124*, 7884−7885.
(88) Chang, C. J.; Yeh, C.-Y.; Nocera, D. G. *J. Org. Chem.* **2002**, *67*, 1403−1406.
(89) Yeh, C.-Y.; Chang, C. J.; Nocera, D. G. *J. Am. Chem. Soc.* **2001**, *123*, 1513−1514.

Scheme 1. Synthesis of Hangman Porphyrins HPX and HPD[a]

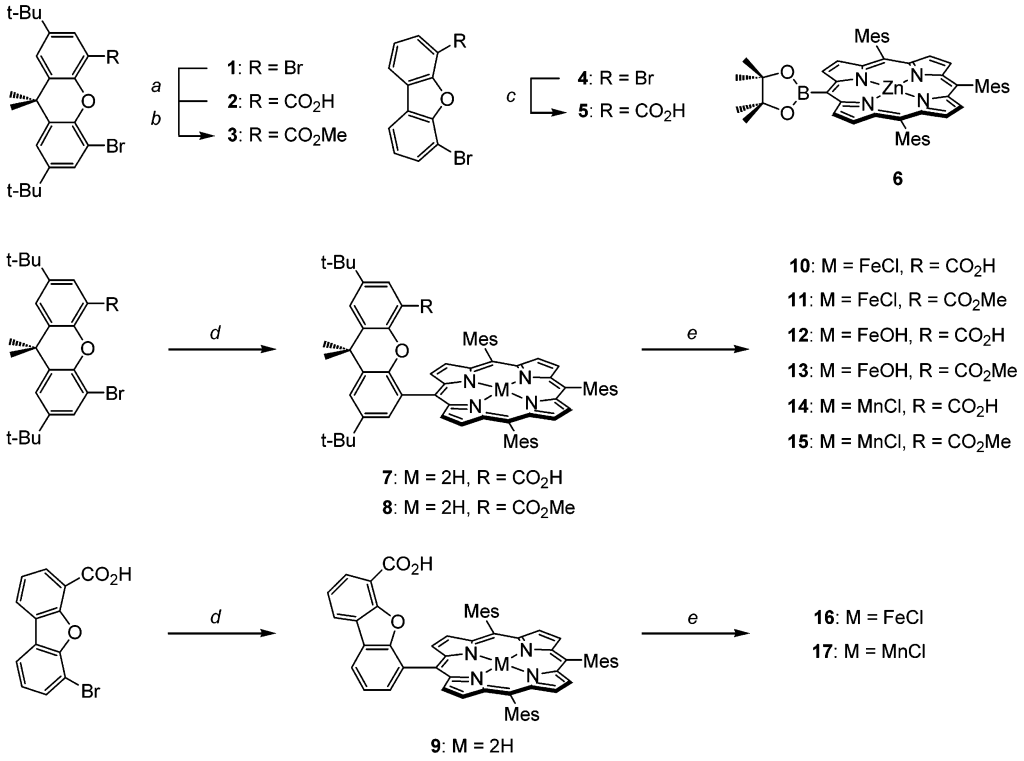

[a] (a) (1) Phenyllithium, cyclohexane/THF, (2) CO_2 gas; (b) methanol, H_2SO_4, reflux; (c) (1) phenyllithium, cyclohexane/THF, (2) CO_2 gas; (d) (1) **6**, Na_2CO_3, $Pd(PPh_3)_4$, DMF/water, reflux, (2) 6 N HCl; (e) (1) $Mn(OAc)_2 \cdot 4H_2O$ or $FeBr_2$, DMF or THF/benzene, reflux, (2) aq NaCl/HCl or aq NaOH.

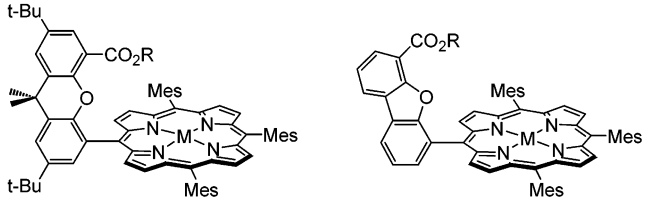

phenyllithium followed by quenching with CO_2 and acid workup furnishes carboxylic acid **2** in 75% yield. Reaction of **2** with H_2SO_4 in methanol affords methyl ester **3** in high yield (93%). 4,6-Dibromodibenzofuran **4** undergoes a similar monolithiation sequence with phenyllithium, CO_2, and acid to give monoacid **5**.

Trimesitylporphyrin boronate **6** is a versatile transmetalating agent for the preparation of HPX and HPD porphyrins.[90,91] Metal-catalyzed cross-couplings of **6** with halide compounds **2**, **3**, or **5** proceed smoothly under typical Suzuki reaction conditions using a $Pd(PPh_3)_4/NaCO_3$ catalyst system. Previously synthesized xanthene-bridged porphyrins bearing a pendant carboxylic acid H_2(HPX-CO_2H) (**7**) or methyl ester H_2(HPX-CO_2Me) (**8**) group are prepared in 72% and 69% yields, respectively. For comparison, macrocycle **8** is prepared in 22% yield under standard Lindsey conditions.[88] Dibenzofuran-bridged porphyrin H_2(HPD-CO_2H) (**9**) is synthesized in 67% yield from **5** and **6**. With the ability to control both the protic capability (carboxylic acid versus ester) and orientation (xanthene versus dibenzoufuran) of the distal hydrogen-bonding functionality, the HPX and HPD platforms provide a set of well-defined molecular scaffolds for systematic examination of proton-coupled O−O bond activation.

Transition-metal complexes of the HPX and HPD systems are readily available from direct reaction with the appropriate metal salt. Iron insertion into HPX porphyrins **7** and **8** with $FeBr_2$ followed by treatment with HCl affords the corresponding chloroiron(III) porphyrin complexes FeCl(HPX-CO_2H) (**10**) and FeCl(HPX-CO_2Me) (**11**) in excellent yields (89% and 92%, respectively). Compounds **10** and **11** were fully characterized by elemental and high-resolution mass spectral analyses. Other metal insertions proceed with equal success. For example, the analogous chloromanganese(III) complexes MnCl(HPX-CO_2H) (**14**) and MnCl(HPX-CO_2Me) (**15**) are prepared in excellent yields (90% and 93%, respectively) by reactions of **7** and **8** with $Mn(OAc)_2 \cdot 4H_2O$ under Alder conditions, followed by workup with NaCl and HCl. Complexes **14** and **15** gave satisfactory high-resolution mass spectral and elemental analyses. The chloroiron(III) FeCl(HPD-CO_2H) (**16**) and chloromanganese(III) MnCl(HPD-CO_2H) (**17**) complexes of HPD are synthesized in a similar way to their HPX congeners in 85% and 90% yield, respectively.

Metalation of **7** and **8** followed by basic workup supplies the monomeric iron(III) hydroxide porphyrins FeOH(HPX-CO_2H) (**12**) and FeOH(HPX-CO_2Me) (**13**) in 92% and 90% yield, respectively. The sterically demanding mesityl groups prevent the formation of bisiron(III) μ-oxo dimers.[92,93] Satisfactory elemental and high-resolution mass spectral analyses accompanied **12** and **13**. The former has been recently charac-

(90) Hyslop, A. G.; Kellett, M. A.; Iovine, P. M.; Therien, M. J. *J. Am. Chem. Soc.* **1998**, *120*, 12676−12677.
(91) Deng, Y.; Chang, C. K.; Nocera, D. G. *Angew. Chem., Int. Ed.* **2000**, *39*, 1066−1068.
(92) Cheng, R.; Latos-Grazynski, L.; Balch, A. L. *Inorg. Chem.* **1982**, *21*, 2412−2418.
(93) Calderwood, T. S.; Bruice, T. C. *Inorg. Chem.* **1985**, *25*, 3722−3724.

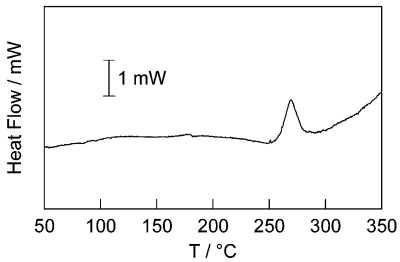

Figure 2. Differential scanning calorimetry (DSC) scan of a solid sample of FeOH(HPX-CO_2H) (**12**) under nitrogen.

terized by single-crystal X-ray analysis.[89] The structure is unique because it is the first monomeric iron(III) hydroxide porphyrin to be analyzed by single-crystal X-ray diffraction analysis,[94] and more significantly, it displays the unprecedented feature of a single structured water molecule. The water is suspended above the heme platform by ditopic hydrogen bonds formed with the distal xanthene carboxylic acid and the terminal hydroxide ligand of the porphyrin. To further probe the properties of the water encapsulated within the hydrogen-bonded scaffold, differential scanning calorimetric (DSC) measurements were undertaken on solid samples of **12**. DSC scans exhibit an endothermic peak with an onset of 270 °C (Figure 2). Thermal gravimetric measurements coupled to in situ infrared absorption detection confirm that this peak corresponds to a dehydration process. The heat flow associated with the dehydration is 21.8 J/g; integration yields a binding energy of 5.8 kcal/mol for the water to the HPX platform. This value attests to the strength of the matched hydrogen-bonding network established by the oxygen atoms of the ditopic metalloporphyrin and the distal carboxylic acid of the Hangman scaffold.

Chemical Generation of High-Valent Ferryl HPX and HPD Derivatives. We sought to provide direct evidence for the formation of high-valent species in order to establish the suitability of the HPX and HPD platforms to effect oxidation reactions. To this end, iron-oxo complexes of the HPX and HPD frameworks analogous to compounds I and II of heme enzymes were prepared at low temperature and spectroscopically interrogated (Figure 3). Chemical oxidation to afford the ferryl porphyrin (compound II) or ferryl porphyrin cation radical (compound III) species is dependent on the axial ligand, solvent, and reaction temperature. Reactions of iron(III) hydroxide complexes **12** and **13** with mCPBA in THF at −61 °C furnish deep red solutions with identical absorption spectra characteristic of neutral iron(IV)-oxo porphyrins, displaying a Soret band at 418 nm ($\epsilon = 170\,000$ M^{-1} cm^{-1}) and a Q-band centered at 555 nm.[93,95] In contrast, treatment of the chloroiron(III) derivatives **10**, **11**, and **16** with PhIO in dichloromethane at −78 °C occurs with the formation of emerald green species, which exhibit absorption spectra consistent with their assignment as iron(IV)-oxo porphyrin cation radicals.[67] These spectra exhibit broadened, blue-shifted Soret bands of decreased molar absorptivity ($\lambda_{max} \sim 406$ nm, $\epsilon \sim 70\,000$ M^{-1} cm^{-1}) with accompanying weak, tailing absorptions at 600−700 nm indicative of porphyrin cation radicals. The successful preparation of high-valent ferryl HPX and HPD complexes presages an oxidation chemistry derived from O−O bond activation chemistry.

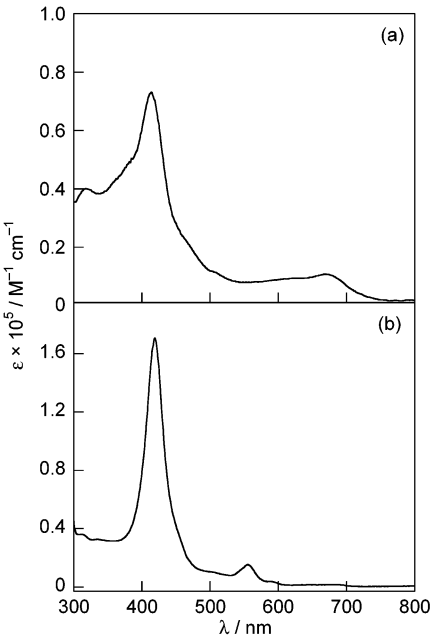

Figure 3. Absorption spectra of high-valent ferryl-HPX complexes analogous to compounds I and II of heme oxygenases. Spectrum (a) was obtained by oxidation of a 10^{-5} M solution of FeCl(HPX-CO_2H) (**10**) with 1.5 equiv of PhIO in dichloromethane at −78 °C. Spectrum (b) was obtained by oxidation of a 10^{-5} M solution of FeOH(HPX-CO_2H) (**12**) with 1.2 equiv of mCPBA in THF at −61 °C.

Catalase-like Disproportionation of Hydrogen Peroxide. Peroxide species offer a direct starting point from which to examine the effects of hydrogen bonding and proton transfer on O−O bond activation chemistry. In nature, catalase enzymes, the majority of which are heme-based, dismutate intracellular hydrogen peroxide to oxygen and water according to the following stoichiometry:[96]

$$2H_2O_2 \xrightarrow{\text{catalase}} O_2 + 2H_2O \qquad (1)$$

Because the 2:1 H_2O_2:O_2 ratio is characteristic of dismutation, we investigated the H_2O_2:O_2 mass balance of eq 1 for the activity of HPX carboxylic acid **10** with H_2O_2 under buffered, biphasic conditions (dichloromethane/aqueous phase, pH 7) in the presence of 1,5-dicyclohexylimidazole at 25 °C. The dioxygen stoichiometry was established by monitoring the release of gas with a buret. Figure 4 displays the yield of O_2 as a function of the initial H_2O_2 concentration in the aqueous layer in the presence of 500 μM **10**. Oxygen is obtained with a linear dependence on the initial concentration of H_2O_2. The slope of the regression line (0.45 ± 0.03) agrees well with the value of 0.5 expected for a catalase-like stoichiometry per eq 1.

A systematic evaluation of catalytic catalase reactivities for the iron HPX and HPD complexes was carried out under the above-mentioned buffered, biphasic conditions. The porphyrin FeCl(TMP) served as a redox-only model compound for baseline comparison. The catalytic results in terms of the turnover numbers (TON) displayed in Figure 5 are striking. Complex **10**, containing a xanthene bridge and a carboxylic acid group, is the most reactive, producing almost an order of magnitude

(94) The structure of a monomeric iron(III)-hydroxide complex of a sterically encumbered porphodimethene has been reported: Buchler, J. W.; Lay, K. L.; Lee, Y. J.; Scheidt, W. R. *Angew. Chem., Int. Ed. Engl.* **1982**, *21*, 432.
(95) Gold, A.; Jayaraj, K.; Doppelt, P.; Weiss, R.; Chottard, G.; Bill, E.; Ding, X.; Trautwein, A. X. *J. Am. Chem. Soc.* **1988**, *110*, 5756−5761.
(96) Nicholls, P.; Fita, I.; Loewen, P. C. *Adv. Inorg. Chem.* **2001**, *51*, 51−106.

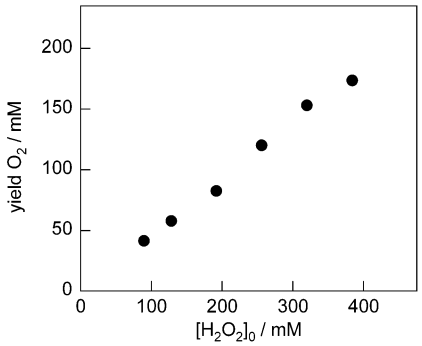

Figure 4. Oxygen release from H_2O_2 dismutation catalyzed by **10** at 25 °C in a biphasic dichloromethane/pH 7 phosphate buffer medium.

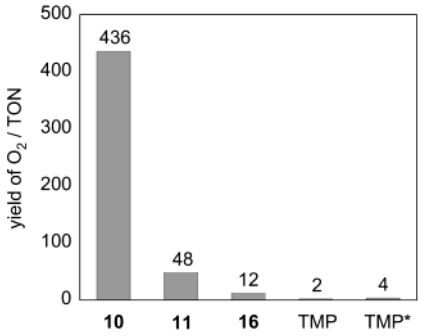

Figure 5. Turnover numbers (TON) for oxygen release from H_2O_2 dismutation catalyzed by iron complexes **10**, **11**, **16**, and FeCl(TMP). In the graph, TMP denotes FeCl(TMP), and TMP* denotes FeCl(TMP) + 1 equiv of benzoic acid.

more oxygen (436 ± 22 TON) than any of the catalysts surveyed. Simple replacement of the "hanging" carboxylic acid group with a methyl ester leads to a significant decrease in catalytic activity (48 ± 3 TON for **11**). Similarly, fixing the carboxylic acid group to the vertically widened dibenzofuran scaffold gives catalytic activities (12 ± 2 for **16**) comparable to those of the baseline compound FeCl(TMP) (2 ± 2).

Several control experiments were performed to verify the foregoing findings. Negligible oxygen evolution is observed in the absence of catalyst or in the presence of catalyst without the axial 1,5-dicyclohexylimidazole ligand. Furthermore, the external addition of 1 equiv of the molecular analogue of the hanging group, either benzoic acid or methyl benzoate, to FeCl(TMP) fails to yield an increase in catalytic catalase activity. Taken together, the data suggest that the protic nature of the hydrogen-bonding group and its orientation are critically important to the efficient activation of the O−O bond by **10**.

Olefin Epoxidation. The success of the HPX-CO_2H system to enhance relative catalase-like activity provided a compelling imperative to extend the reactivity of the Hangman platforms to other processes contingent on O−O bond activation. We targeted the catalytic epoxidation of olefins (eq 2) using hydrogen peroxide as a terminal oxidant for the following reasons. First, the reaction parallels the peroxide shunt cycle[36,37,43] of cytochrome P450 and peroxidase enzymes while building on the results of the observed biomimetic catalase activity. Second, hydrogen peroxide is a green oxidant, yielding water as the sole byproduct of catalysis.

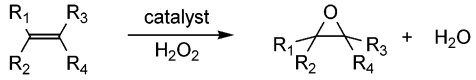

(2)

Table 1. Epoxidation of Olefins Catalyzed by Manganese Complexes **14**, **15**, **17**, and MnCl(TMP)[a]

Catalyst	Substrate	
	Styrene (% yield)	*Cis*-cyclooctene(% yield)
MnC1(HPX-CO_2H) (**14**)	70 ± 2	92 ± 6
MnC1(HPX-CO_2Me) (**15**)	38 ± 2	42 ± 5
MnC1(HPD-CO_2H) (**17**)	4 ± 1	5 ± 1
MnC1(TMP)	4 ± 2	5 ± 1
MnC1(TMP) + 1 equiv PhCOOH	6 ± 1	9 ± 2

[a] Standard catalytic reaction conditions are given in the Experimental Section. Yields were determined by analysis of the epoxide products by GC-MS.

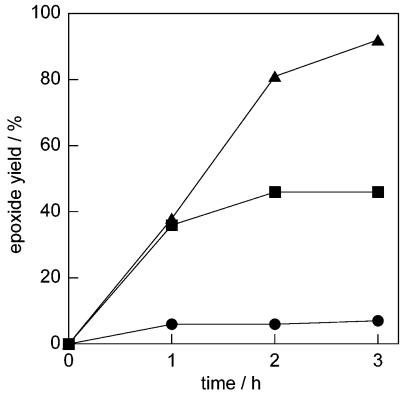

Figure 6. Time-course plot for the epoxidation of *cis*-cyclooctene with hydrogen peroxide catalyzed by **14** (▲), **15** (■), and MnCl(TMP) (●). The addition of 1 equiv of benzoic acid to MnCl(TMP) shows no detectable enhancement in catalytic epoxidation reactivity.

Initial catalytic olefin epoxidation studies with the iron Hangman porphyrins using a H_2O_2/1,5-dicyclohexylimidazole system were unsuccessful, owing to the electron-rich nature of both the porphyrin and the axial ligand.[97] We thus turned our attention to the reactivity of the manganese HPX and HPD derivatives **14**, **15**, and **17**, with MnCl(TMP) as the standard baseline compound. The common olefins styrene and *cis*-cyclooctene were chosen as substrates. Table 1 lists the product yields for olefin epoxidation with H_2O_2 catalyzed by the manganese complexes at 0.2 mol % catalyst loading, and Figure 6 presents a time-course plot for the epoxidation reactions catalyzed by **14**, **15**, and MnCl(TMP). Epoxide products are formed in >95% selectivity with little to no allylic oxidation side products, indicating that the involvement of radical species such as HO· and HOO· are unlikely.[67,98] The results for epoxidation reactivity of the manganese derivatives follow the same general trend observed for the iron-mediated catalase reactions. Complex **14** bearing a protic carboxylic acid group on a xanthene platform is the most active, affording styrene and *cis*-cyclooctene oxides in 70% (350 ± 10 TON) and 92% (460 ± 30 TON) yields, respectively. These values are almost twice as high as those obtained for the ester derivative **15** (191 ± 8 TON for styrene, 208 ± 22 TON for *cis*-cyclooctene). Under these conditions, both HPD complex **17** and MnCl(TMP) yield significantly less epoxide product upon reaction with either styrene or *cis*-cyclooctene (<10%, <50 TON). As observed for

(97) Nam and co-workers have used a combination of electron-deficient imidazole co-ligands and electron-rich iron(III) porphyrins to catalyze olefin epoxidation with H_2O_2: Nam, W.; Lee, H. J.; Oh, S.-Y.; Kim, C.; Jang, H. G. *J. Inorg. Biochem.* **2000**, *80*, 219−225.

(98) Sheldon, R. A. *Metalloporphyrins in Catalytic Oxidations*; Marcel Dekker: New York, 1994.

the catalase reactions, negligible olefin epoxidation is detected in the absence of catalyst or in the presence of catalyst without axial ligand. Furthermore, the external addition of 1 equiv of either benzoic acid or methyl benzoate to MnCl(TMP) fails to yield an increase in epoxide product. Last, we also examined the stereochemistry of the epoxidation of *cis*-stilbene by **14**.[99−102] The high *cis*-epoxide/*trans*-epoxide ratio of 6 ± 1 obtained is consistent with a predominant oxomanganese(V) porphyrin oxidizing agent.[103−106]

Discussion

Specific and efficient catalytic oxidation chemistry in heme-dependent proteins is made possible by the ability of these enzymes to exquisitely balance proton and electron inventories. In particular, the distal side of the heme is crucial for providing a suitable microenvironment surrounding the open coordination site of the heme for the binding of peroxides, molecular oxygen, and other small-molecule substrates and controlling their subsequent catalytic chemistry as derived from coupled proton and electron transfer. For peroxidases, catalases, and the cytochrome P450 monooxygenases, such PCET events facilitate the selective heterolytic cleavage of O−O bonds via the pull effect to form high-valent iron-oxo porphyrin species such as compound I [ferryl (Fe^{IV}═O) species paired with a porphyrin cation radical] for further reaction with external substrates.[36−39] The key O−O cleavage step itself is driven by proton activation of a hydroperoxide intermediate, which occurs by a hydrogen-bonding shuttle derived from proximate amino acids and/or directed water.

The reaction chemistry of these natural enzymes emphasizes the importance of managing proton inventory in catalytic oxidation processes. Heretofore, metalloporphyrins employed as models for heme-mediated oxidation chemistry have, for the most part, focused on either modifying the redox or steric properties of the macrocycle itself or changing the electronic identity of the proximal axial ligand.[98,107] Few intermolecular small-molecule model systems have emerged that attend to issues surrounding the pull effect. Notable exceptions include Traylor's studies of the general acid−base effects of added imidazole in the catalytic oxidation of phenols using iron porphyrins and peracid or hydroperoxide oxidants[108−110] and Bruice's reports of the effects of imidazole and pH on similar O−O cleavage reactions catalyzed by metalloporphyrins in aqueous solution.[111−113] More recently, Nam and co-workers address the complexities of homolytic versus heterolytic O−O bond cleavage pathways in protic and aprotic solvents[114,115] and demonstrate remarkable spectator ligand effects in metalloporphyrin-catalyzed oxidation reactions.[116,117] In no case, however, has the simple metalloporphyrin model system been designed to intramolecularly control the proton inventory for small-molecule activation reactivity.[118−126] In doing so per a Hangman strategy, catalytic bond-making and bond-breaking chemistry on the metalloporphyrin redox platform is significantly enhanced. These systems isolate the key proton-shuttle attribute of the distal heme cleft in a tunable synthetic platform by scaffolding a single hydrogen-bonding group over a heme core. This small-molecule approach affords the ability to control the acid−base properties of the hydrogen-bonding functionality by direct synthetic modification. Moreover, the spatial orientation of this hydrogen-bonding distal group in relation to the porphyrin redox platform can be modified by choice of either the xanthene or dibenzofuran scaffold.

Structure−reactivity relationships of the HPX and HPD frameworks in catalase-like hydrogen peroxide dismutations and peroxide-mediated olefin epoxidations reveal that both the nature and spatial orientation of the hydrogen-bonding group are critical for selective and efficient catalytic chemistry. Substitution of an aprotic hydrogen-bonding ester group for the protic carboxylic acid on the HPX platform results in catalyst architectures with significantly diminished activity for the former. Moreover, the catalytic studies reveal that the arrangement of acid−base and redox sites is also vital for oxidation reactivity. From the previously reported structure of **12**, the monomeric iron(III) derivative of the HPX-CO_2H ligand has the unique ability to juxtapose two oxygen atoms between proton (carboxylic acid) *and* electron (metalloporphyrin) shuttle sites. Thus, the HPX template provides a geometrically matched microcavity for the binding and activation of peroxide and other reactive oxygen species.

The divergent oxidation reactivities displayed by the Hangman systems can be grouped into a unified mechanistic model that falls within the framework of natural heme enzyme reactivity. The proposed catalytic pathway for the O−O reactivity of the most active xanthene-bridged HPX-CO_2H platform is shown in Scheme 2. Reaction of H_2O_2 with the porphyrin in the presence of an axial ligand results in a putative

(99) Groves, J. T.; Stern, M. K. *J. Am. Chem. Soc.* **1988**, *110*, 8628−8638.
(100) Bortolini, O.; Meunier, B. *J. Chem. Soc., Perkin Trans. 2* **1984**, 1967−1970.
(101) Battioni, P.; Renaud, J. P.; Bartoli, J. F.; Reina-Artiles, M.; Fort, M.; Mansuy, D. *J. Am. Chem. Soc.* **1988**, *110*, 8462−8470.
(102) Castellino, A. J.; Bruice, T. C. *J. Am. Chem. Soc.* **1988**, *110*, 158−162.
(103) Jin, N.; Bourassa, J. L.; Tizio, S. C.; Groves, J. T. *Angew. Chem., Int. Ed.* **2000**, *39*, 3849−3851.
(104) Jin, N.; Groves, J. T. *J. Am. Chem. Soc.* **1999**, *121*, 2923−2924.
(105) Nam, W.; Kim, I.; Lim, M. H.; Choi, H. J.; Lee, J. S.; Jang, H. G. *Chem. Eur. J.* **2002**, *8*, 2067−2071.
(106) Gross has recently characterized oxomanganese(V) corroles: Gross, Z.; Golubkov, G.; Simkovich, L. *Angew. Chem., Int. Ed.* **2000**, *39*, 4045−4047.
(107) Kadish, K. M.; Smith, K. M.; Guilard, R. *The Porphyrin Handbook*; Academic Press: San Diego, CA, 2000; and references therein.
(108) Traylor, T. G.; Lee, W. A.; Stynes, D. V. *J. Am. Chem. Soc.* **1984**, *106*, 755−764.
(109) Traylor, T. G.; Ciccone, J. P. *J. Am. Chem. Soc.* **1989**, *111*, 8413−8420.
(110) Traylor, T. G.; Xu, F. *J. Am. Chem. Soc.* **1990**, *112*, 178−186.
(111) Lee, W. A.; Bruice, T. C. *J. Am. Chem. Soc.* **1985**, *107*, 513−514.
(112) Zipplies, M. F.; Lee, W. A.; Bruice, T. C. *J. Am. Chem. Soc.* **1986**, *108*, 4433−4445.
(113) Bruice, T. C.; Balasubramanian, P. N.; Lee, R. W.; Smith, J. R. L. *J. Am. Chem. Soc.* **1988**, *110*, 7890−7892.
(114) Nam, W.; Lim, M. L.; Moon, S. K.; Kim, C. *J. Am. Chem. Soc.* **2000**, *122*, 10805−10809.
(115) Nam, W.; Han, H. J.; Oh, S.-Y.; Lee, Y. J.; Choi, M.-H.; Han, S.-Y.; Kim, C.; Woo, S. K.; Shin, W. *J. Am. Chem. Soc.* **2000**, *122*, 8677−8684.
(116) Nam, W.; Jin, S. W.; Lim, M. H.; Ryu, J. Y.; Kim, C. *Inorg. Chem.* **2002**, *41*, 3647−3652.
(117) Nam, W.; Lim, M. H.; Oh, S.-Y.; Lee, J. H.; Lee, H. J.; Woo, S. K.; Kim, C.; Shin, W. *Angew. Chem., Int. Ed.* **2000**, *39*, 3646−3649.
(118) For some seminal studies describing hydrogen-bonded porphyrins for the binding and transport of dioxygen and carbon monoxide, see refs 119−126.
(119) Chang, C. K.; Kondylis, M. P. *J. Chem. Soc., Chem. Commun.* **1986**, 316−318.
(120) Chang, C. K.; Liang, Y.; Aviles, G.; Peng, S.-M. *J. Am. Chem. Soc.* **1995**, *117*, 4191−4192.
(121) Collman, J. P.; Fu, L. *Acc. Chem. Res.* **1999**, *32*, 455−463.
(122) Momenteau, M.; Reed, C. A. *Chem. Rev.* **1994**, *94*, 659−698.
(123) Gerothanassis, I. P.; Momenteau, M.; Loock, B. *J. Am. Chem. Soc.* **1989**, *111*, 7006−7012.
(124) Wuenschell, G. E.; Tetreau, C.; Lavalette, D.; Reed, C. A. *J. Am. Chem. Soc.* **1992**, *114*, 3346−3355.
(125) Walker, F. A.; Bowen, J. *J. Am. Chem. Soc.* **1985**, *107*, 7632−7635.
(126) Tani, F.; Matsu-Ura, M.; Nakayama, S.; Naruta, Y. *Coord. Chem. Rev.* **2002**, *226*, 219−226.

Scheme 2. Proposed Pathway for Proton-Assisted Metal-Oxo Formation and Substrate Oxidation by HPX Hangman Porphyrins

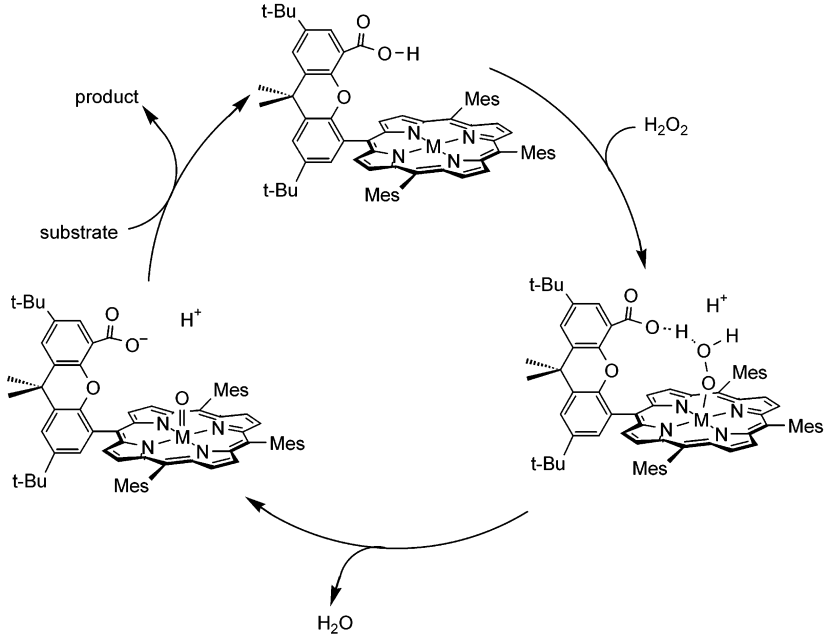

metal hydroperoxide complex. The bound HO_2^- species is then converted into an oxoiron(IV) porphyrin cation radical or an oxomanganese(V) intermediate by proton transfer and subsequent heterolytic O−O bond cleavage. The high-valent metal-oxo species generated are sufficiently reactive to oxidize substrates. Alternatively, protonation activates the hydroperoxide for direct reaction with substrates prior to O−O bond cleavage. Increasing the distance between the ditopic sites by use of a dibenzofuran-based HPD scaffold affords a catalyst that has comparable performance to a simple tetramesitylporphyrin counterpart, despite the presence of a pendant protic hydrogen-bonding group. It is tempting to suggest that the control of proton transfer in these catalytic cycles avoids homolytic cleavage or other peroxide decomposition pathways, and ongoing mechanistic work is aimed at addressing such issues.

The pull-based mechanism provides a working model for assessing the relative reactivities of the Hangman platforms by inspection of the key metal-hydroperoxide intermediate. The HPX-CO_2H system, which exhibits the highest reactivity, has the capacity to stabilize binding of the oxidant by hydrogen bonding, while the carboxylic acid group provides an intramolecular shuttle to deliver proton equivalents for oxidation chemistry. The ester derivative HPX-CO_2Me can also stabilize a bound HO_2^- species via hydrogen bonding through its hanging carbonyl group but is unable to offer an internal pathway for protons. Finally, the comparable activities of the HPD-CO_2H and TMP series suggest that hydrogen bonding and intramolecular proton transfer are inefficient in the former, owing to the splayed arrangement of redox and acid−base sites.

Concluding Remarks

The present work represents an initial study to utilize PCET as a mechanistic framework for exploring small-molecule activation chemistry. Our findings clearly indicate that the introduction of a single proton-shuttle group onto a redox-active platform in simple chemical model systems can significantly affect the activation of O−O bonds for disparate catalytic processes. We stress here that our aim is not to create competitive analogues of existing catalysts but to demonstrate how the addition of proton control can enhance the reactivity of a redox cofactor. To this end, the catalytic processes of the catalase-like disproportionation of hydrogen peroxide and the epoxidation of olefins have been compared for the HPX and HPD systems and redox-only porphyrin platforms. For both cases, a marked activity enhancement is observed for the xanthene-bridged platform with a pendant carboxylic acid group (HPX-CO_2H), which features a geometrically matched site between proton and electron sources. The reactivity data establish that this Hangman approach can yield superior catalysts to analogues that do not manage both proton and electron inventories.

The results have significant implications from the perspectives of both biological enzymes and catalyst design. First, the ability to achieve efficient catalase or epoxidation reactivity with a single metalloporphyrin-based scaffold is evocative of natural heme-dependent proteins that employ a conserved protoporphyrin IX cofactor to effect a myriad of chemical reactivities. In terms of synthetic catalyst design, the Hangman strategy demonstrates that the addition of proton control to a redox platform can enhance its catalytic performance. The importance of hydrogen bonding for controlling oxygen activation has been emphasized recently with the *stoichiometric* reactions of oxygen and water within tripodal non-heme cavities.[127−133] The Hangman approach described here is distinguished by its ability to use a hydrogen-bond network to actively deliver protons to drive

(127) MacBeth, C. E.; Golombek, A. P.; Young, V. G., Jr.; Tang, C.; Kuczera, K.; Hendrich, M. P.; Borovik, A. S. *Science* **2000**, *289*, 938−941.
(128) Gupta, R.; MacBeth, C. E.; Young, V. G., Jr.; Borovik, A. S. *J. Am. Chem. Soc.* **2002**, *124*, 1136−1137.
(129) Hammes, B. S.; Young, V. G., Jr.; Borovik, A. S. *Angew. Chem., Int. Ed.* **1999**, *38*, 666−669.
(130) Wada, A.; Ogo, S.; Nagatomo, S.; Kitagawa, T.; Watanbe, Y.; Jitsukawa, K.; Masuda, H. *Inorg. Chem.* **2002**, *41*, 616−618.
(131) Ogo, S.; Wada, S.; Watanbe, Y.; Iwase, M.; Wada, A.; Harata, M.; Jitsukawa, K.; Masuda, H.; Einaga, H. *Angew. Chem., Int. Ed.* **1998**, *37*, 2102−2104.
(132) Garner, D. K.; Allred, R. A.; Tubbs, K. J.; Arif, A. M.; Berreau, L. M. *Inorg. Chem.* **2002**, *41*, 3533−3541.
(133) Berreau, L. M.; Mahapatra, S.; Halfen, J. A.; Young, V. G., Jr.; Tolman, W. B. *Inorg. Chem.* **1996**, *35*, 6339−6342.

catalytic oxygen activation processes. We anticipate that the further development of hybrid architectures containing both acid−base and redox functionalities will lead to new advances in catalysis. In this vein, current work is directed at the synthesis of platforms that will permit, by transient absorption spectroscopy, direct mechanistic investigations of the proton-coupled O−O activation process and platforms that will expand the scope of multielectron PCET reactions associated with catalytic bond-making and bond-breaking chemistry.

Experimental Section

Materials. Silica gel 60 (70−230 and 230−400 mesh, Merck) and aluminum oxide 60 (EM Science) were used for column chromatography. Analytical thin-layer chromatography was performed on JT Baker IB-F silica gel (precoated sheets, 0.2 mm thick) or JT Baker IB-F aluminum oxide (precoated sheets, 0.2 mm thick). Solvents for synthesis were reagent-grade or better and were dried according to standard methods.[134] 4,5-Dibromo-2,7-di-*tert*-butyl-9,9-dimethylxanthene **1**,[135] 4,6-dibromodibenzofuran **4**,[136] and 4-bromo-6-hydroxycarbonyldibenzofuran **5**[136] were prepared according to literature procedures. The reference porphyrins FeCl(TMP) and MnCl(TMP) are available by published protocols.[107] The preparation of zinc(II) 5,10,15-trimesityl-20-(4′,4′,5′,5′-tetramethyl[1′,3′,2′] dioxaborolan-2′-yl)porphyrin (**6**) will be detailed in a future report. All other reagents were used as received.

4-Hydroxycarbonyl-5-bromo-2,7-di-*tert*-butyl-9,9-dimethylxanthene (2). Phenyllithium (1.2 mL, 1.8 M solution in cyclohexane) was added over a period of 10 min to a solution of xanthene dibromide **1** (1.00 g, 2.08 mmol) in dry THF (40 mL) cooled to −78 °C under a nitrogen atmosphere. After the mixture was stirred at −78 °C under nitrogen for 1 h, CO_2 gas was bubbled into the lithiate at a rapid rate until the yellow color of the solution had faded. The mixture was then allowed to warm to room temperature and stirred overnight. The reaction was quenched with 2 N HCl (15 mL) and the organic solvent was removed by rotary evaporation. The resulting white precipitate was filtered and washed with water. Purification by column chromatography (silica gel, dichloromethane) delivered **2** as a white powder (0.7 g, 75% yield). ^{1}H NMR (500 MHz, $CDCl_3$, 25 °C): δ = 8.18 (d, J = 4 Hz, 1H, ArH), 7.66 (d, J = 4 Hz, 1H, ArH), 7.50 (d, J = 4 Hz, 1H, ArH), 7.40 (d, J = 4 Hz, 1H, ArH), 1.68 (s, 6H, CH_3), 1.37 (s, 9H, CH_3), 1.35 (s, 9H, CH_3).

4-Methoxycarbonyl-5-bromo-2,7-di-*tert*-butyl-9,9-dimethylxanthene (3). A solution of acid **2** (1.0 g, 2.53 mmol) in methanol (50 mL) and H_2SO_4 (2 mL) was refluxed for 4 h. The solvent was removed in vacuo, water (20 mL) was added to the residue, and the resulting precipitate was filtered. The solid was redissolved in dichloromethane (50 mL), washed with 15% HCl and water, dried over Na_2SO_4, and taken to dryness by rotary evaporation. Purification by column chromatography (silica gel, dichloromethane) provided ester **3** as a white powder (0.96 g, 93% yield). ^{1}H NMR (500 MHz, $CDCl_3$, 25 °C): δ = 7.72 (d, J = 4 Hz, 1H, ArH), 7.55 (d, J = 4 Hz, 1H, ArH), 7.46 (d, J = 4 Hz, 1H, ArH), 7.32 (d, J = 4 Hz, 1H, ArH), 4.02 (s, 3H, CH_3), 1.64 (s, 6H, CH_3), 1.35 (s, 9H, CH_3), 1.33 (s, 9H, CH_3).

5-[4-(5-Hydroxycarbonyl-2,7-di-*tert*-butyl-9,9-dimethylxanthenyl)]-10,15,20- trimesitylporphyrin, H_2(HPX-CO_2H) (7). Under a nitrogen atmosphere, solids **2** (30 mg, 0.067 mmol), **6** (68 mg, 0.080 mmol), Na_2CO_3 (25 mg), and $Pd(PPh_3)_4$ (15 mg, 0.0130 mmol) were combined in a 50-mL Schlenk flask. DMF (10 mL) and deionized water (1 mL) were added, and the mixture was heated at reflux overnight under nitrogen. The reaction was taken to dryness and the residue was redissolved in dichloromethane (25 mL), stirred with 6 N HCl (25 mL) for 30 min, and washed with water (7 × 25 mL). The organic layer was separated and dried over Na_2SO_4, and the solvent was removed by rotary evaporation. Purification by column chromatography (silica gel, 2:1 hexanes/dichloromethane to dichloromethane) followed by recrystallization from dichloromethane/methanol solutions delivered **7** as a royal purple powder (50 mg, 72% yield). Complex **7** obtained by this synthetic method gave comparable high-resolution mass spectral and elemental analyses to batches prepared by Lindsey cyclizations.

5-[4-(5-Methoxycarbonyl-2,7-di-*tert*-butyl-9,9-dimethylxanthenyl)]-10,15,20- trimesitylporphyrin, H_2(HPX-CO_2Me) (8). Under a nitrogen atmosphere, solids **3** (30 mg, 0.065 mmol), **6** (68 mg, 0.080 mmol), Na_2CO_3 (25 mg), and $Pd(PPh_3)_4$ (15 mg, 0.0130 mmol) were combined in a 50-mL Schlenk flask. DMF (10 mL) and deionized water (1 mL) were added, and the mixture was heated at reflux overnight under nitrogen. The reaction was taken to dryness and the residue was redissolved in dichloromethane (25 mL), stirred with 6 N HCl (25 mL) for 30 min, and washed with water (7 × 25 mL). The organic layer was separated and dried over Na_2SO_4, and the solvent was removed by rotary evaporation. Purification by column chromatography (silica gel, 2:1 hexanes/dichloromethane) delivered **8** as a royal purple powder (47 mg, 69% yield). Complex **8** obtained by this synthetic method gave comparable high-resolution mass spectral and elemental analyses to batches prepared by Lindsey cyclizations.

5-[4-[6-(Hydroxycarbonyl)dibenzofuranyl]]-10,15,20-trimesitylporphyrin, H_2(HPD-CO_2H) (9). Under a nitrogen atmosphere, a mixture of 6-bromo-4-dibenzofurancarboxylic acid (**5**) (42 mg, 0.144 mmol), **6** (135 mg, 0.159 mmol), Na_2CO_3 (49 mg, 0.462 mmol), and $Pd(PPh_3)_4$ (25 mg, 0.0216 mmol) were combined in a Schlenk flask. DMF (20 mL) and deionized water (2 mL) were added, and the mixture was refluxed for 19 h under nitrogen. The solvent was removed and the residue was redissolved in dichloromethane (30 mL) and stirred with 6 N HCl (20 mL) for 30 min. The organic layer was separated and washed with 20% aqueous Na_2CO_3 (20 mL) followed by water (2 × 50 mL). The solvent was evaporated and the residue was purified by column chromatography (silica gel, 2:1 hexanes/dichloromethane to 1:1 ethyl acetate/dichloromethane) to afford **9** as a purple solid (85 mg, 67% yield). ^{1}H NMR (300 MHz, $CDCl_3$, 25 °C): δ = 8.66 (m, 8H), 8.41 (m, 2H), 8.30 (dd, J_1 = 7.6 Hz, J_2 = 1.3 Hz, 1H), 8.06 (dd, J_1 = 7.8 Hz, J_2 = 1.3 Hz, 1H), 7.85 (t, J = 7.6 Hz, 1H), 7.52 (t, J = 7.8 Hz, 1H), 7.30 (s, 1H), 7.29 (s, 1H), 7.26 (s, 4H), 2.65 (s, 3H), 2.62 (s, 6H), 1.91 (s, 3H), 1.88 (s, 9H), 1.87 (s, 6H), −2.46 (s, 2H). HRESIMS (MH^+) m/z calcd for $C_{60}H_{51}N_4O_3$ 875.3956, found 875.3969.

FeCl(HPX-CO_2H) (10). A combination of **7** (218 mg, 0.21 mmol), $FeBr_2$ (270 mg), and DMF (35 mL) was refluxed under nitrogen for 2 h, opened to air, and brought to dryness under vacuum. The solids were redissolved in dichloromethane (100 mL) and washed with water (4 × 75 mL). The organic layer was stirred with 20% HCl (50 mL) for 75 min, washed with water (5 × 100 mL), and taken to dryness. The resulting residue was purified by column chromatography (silica gel, dichloromethane to 5% methanol/dichloromethane), and retreated with HCl as described above to furnish **10** as a brown powder (211 mg, 89% yield). HRFABMS ($[M - Cl]^+$) m/z calcd for $C_{71}H_{70}N_4O_3$Fe, 1082.4797; found, 1082.4773. Anal. Calcd for $C_{71}H_{70}ClN_4O_3$Fe: C, 76.23; H, 6.31; N, 5.01. Found: C, 76.44; H, 6.19; N, 4.82.

FeCl(HPX-CO_2Me) (11). In a drybox, **8** (50 mg, 0.048 mmol), 2,6-lutidine (0.1 mL), $FeBr_2$ (100 mg), and THF (15 mL) were loaded in a 100-mL flask equipped with a condenser. The reaction was refluxed under nitrogen for 5 h, opened to air, and brought to dryness under vacuum. The residue was purified by column chromatography (silica gel, dichloromethane to 10% methanol/dichloromethane), redissolved in dichloromethane (50 mL), and stirred with 20% HCl (25 mL) for 1 h. The organic layer was washed with water (5 × 50 mL) and taken to dryness. The resulting residue was purified by column chromatography (silica gel, dichloromethane to 5% methanol/dichloromethane), and retreated with HCl as described above to furnish **11** as a brown powder (50 mg, 92% yield). HRFABMS ($[M - Cl]^+$) m/z calcd for $C_{72}H_{72}N_4O_3$-

(134) Armarego, W. L. F.; Perrin, D. D. *Purification of Laboratory Chemicals*, 4th ed.; Butterworth-Heinmann: Oxford, U.K., 1996.
(135) Nowick, J. S.; Ballester, P.; Ebmeyer, F.; Rebek, J., Jr. *J. Am. Chem. Soc.* **1990**, *112*, 8902−8906.
(136) Schwartz, E. B.; Knobler, C. B.; Cram, D. J. *J. Am. Chem. Soc.* **1992**, *114*, 10775−10784.

Fe, 1096.4954; found, 1096.4969. Anal. Calcd for $C_{72}H_{72}ClN_4O_3Fe$: C, 76.35; H, 6.41; N, 4.95. Found: C, 76.70; H, 6.72; N, 4.62.

FeOH(HPX-CO_2H) (12). A combination of **7** (218 mg, 0.21 mmol), $FeBr_2$ (270 mg), and DMF (35 mL) was refluxed under nitrogen for 2 h, opened to air, and brought to dryness under vacuum. The solids were redissolved in dichloromethane (100 mL) and washed with water (4 × 75 mL). The organic layer was stirred with 20% HCl (50 mL) for 75 min, washed with water (5 × 100 mL), and taken to dryness. The resulting residue was purified by column chromatography (silica gel, dichloromethane to 1% methanol/dichloromethane), redissolved in toluene (100 mL), and stirred with 0.5 M NaOH (100 mL) for 12 h. The organic layer was washed with water (3 × 50 mL) and dried over Na_2SO_4. Removal of the solvent followed by recrystallization from pentane afforded analytically pure **12** as a brown microcrystalline powder (212 mg, 92% yield). HRFABMS ($[M - OH]^+$) *m*/*z* calcd for $C_{71}H_{70}N_4O_3Fe$, 1082.4797; found, 1082.4824. Anal. Calcd for $C_{76}H_{85}N_4O_5Fe$: C, 76.68; H, 7.20; N, 4.71. Found: C, 76.78; H, 7.19; N, 4.69.

FeOH(HPX-CO_2Me) (13). In a drybox, **8** (50 mg, 0.040 mmol), 2,6-lutidine (0.1 mL), $FeBr_2$ (100 mg), and THF (15 mL) were loaded in a 100-mL flask equipped with a condenser. The reaction was refluxed under nitrogen for 5 h, opened to air, and brought to dryness under vacuum. The residue was purified by column chromatography (silica gel, dichloromethane to 10% methanol/dichloromethane), redissolved in dichloromethane (50 mL), and stirred with 20% HCl (25 mL) for 1 h. The organic layer was washed with water (5 × 50 mL) and taken to dryness. The resulting solid was redissolved in toluene (50 mL) and stirred with 0.5 M NaOH (50 mL) for 12 h. The organic phase was washed with water (3 × 50 mL) and dried over Na_2SO_4, and the solvent was removed by rotary evaporation. Recrystallization from pentane furnished analytically pure **13** as a brown powder (48 mg, 90% yield). HRFABMS ($[M - OH]^+$) *m*/*z* calcd for $C_{72}H_{72}N_4O_3Fe$, 1096.4954; found, 1096.4982. Anal. Calcd for $C_{77}H_{87}N_4O_5Fe$: C, 76.79; H, 7.28; N, 4.65. Found: C, 76.74; H, 7.36; N, 4.72.

MnCl(HPX-CO_2H) (14). A solution of **7** (103 mg, 0.10 mmol) and $Mn(OAc)_2 \cdot 4H_2O$ (220 mg) in DMF (15 mL) was refluxed in air for 3 h. The reaction was cooled to room temperature and taken to dryness. The remaining residue was taken up in a 1:1 mixture of dichloromethane/water (50 mL). The organic layer was separated, washed with water (3 × 75 mL), and stirred with a 5:1 mixture of saturated aqueous NaCl and HCl (72 mL) for 90 min. The organic layer was decanted, and the solvent was removed under vacuum. The remaining solid was purified by column chromatography (silica gel, dichloromethane to 5% methanol/dichloromethane) and retreated with aqueous NaCl and HCl as described above. The organic phase was separated, washed with water (3 × 75 mL), dried over Na_2SO_4, and taken to dryness. Recrystallization from dichloromethane and hexanes afforded pure **14** as a forest green microcrystalline powder (101 mg, 90% yield). HRFABMS ($[M - Cl]^+$) *m*/*z* calcd for $C_{71}H_{70}N_4O_3Mn$, 1081.4828; found, 1081.4833. Anal. Calcd for $C_{71}H_{70}ClN_4O_3Mn$: C, 76.29; H, 6.31; N, 5.01. Found: C, 76.37; H, 6.14; N, 4.93.

MnCl(HPX-CO_2Me) (15). A solution of **8** (103 mg, 0.098 mmol) and $Mn(OAc)_2 \cdot 4H_2O$ (220 mg) in DMF (15 mL) was refluxed in air for 3 h. The reaction was cooled to room temperature and taken to dryness. The remaining residue was taken up in a 1:1 mixture of dichloromethane/water (50 mL). The organic layer was separated, washed with water (3 × 75 mL), and stirred with a 5:1 mixture of saturated aqueous NaCl and HCl (72 mL) for 90 min. The organic layer was decanted, and the solvent was removed under vacuum. The remaining solid was purified by column chromatography (silica gel, dichloromethane to 5% methanol/dichloromethane) and retreated with aqueous NaCl and HCl as described above. The organic phase was separated, washed with water (3 × 75 mL), dried over Na_2SO_4, and taken to dryness. Recrystallization from dichloromethane and hexanes afforded pure **15** as a hunter green powder (102 mg, 93% yield). HRFABMS ($[M - Cl]^+$) *m*/*z* calcd for $C_{72}H_{72}N_4O_3Mn$, 1095.4985; found, 1095.4973. Anal. Calcd for $C_{72}H_{72}ClN_4O_3Mn$: C, 76.41; H, 6.41; N, 4.95. Found: C, 76.32; H, 6.32; N, 5.05.

FeCl(HPD-CO_2H) (16). Iron insertion into the free base porphyrin was achieved by a standard literature procedure. A mixture of **9** (15 mg, 0.0171 mmol), $FeBr_2$ (37 mg, 0.171 mmol), and anhydrous DMF (3.5 mL) was refluxed under nitrogen for 2 h, opened to air, and brought to dryness under vacuum. The residue was redissolved in dichloromethane (10 mL) and washed with water (3 × 30 mL). The organic layer was stirred with 20% HCl (4 mL) for 75 min, washed with water (3 × 30 mL), and taken to dryness. The residue was purified by column chromatography (silica gel, dichloromethane to 10% methanol/dichloromethane), redissolved in dichloromethane (10 mL), and stirred with 4 N HCl (1.5 mL) overnight. The organic layer was separated, washed with water (3 × 40 mL), dried over Na_2SO_4, and evaporated. The iron complex **16** was isolated as a brown powder (14 mg, 85% yield). HRESIMS ($[M - Cl]^+$) *m*/*z* calcd for $C_{60}H_{48}N_4O_3Fe$, 928.3070; found, 928.3064.

MnCl(HPD-CO_2H) (17). A solution of **9** (15 mg, 0.0171 mmol) and $Mn(OAc)_2 \cdot 4H_2O$ (30 mg) in DMF (5 mL) was refluxed in air for 3 h. The reaction was cooled to room temperature and taken to dryness. The residue was taken up in a 1:1 mixture of dichloromethane/water (25 mL). The organic layer was separated, washed with water (3 × 25 mL), and stirred with a 5:1 mixture of saturated aqueous NaCl and HCl (24 mL) for 90 min. The organic layer was decanted, and the solvent was removed under vacuum. The remaining solid was purified by column chromatography (silica gel, dichloromethane to 5% methanol/dichloromethane) and retreated with aqueous NaCl and HCl as described above. The organic phase was separated, washed with water (3 × 25 mL), dried over Na_2SO_4, and taken to dryness. Recrystallization from dichloromethane and hexanes afforded pure **17** as a green solid (15 mg, 90% yield). HRESIMS ($[M - Cl]^+$) *m*/*z* calcd for $C_{60}H_{48}N_4O_3Mn$, 927.3101; found 927.3093.

Physical Measurements. ^{1}H NMR spectra were collected in $CDCl_3$ or toluene-d_8 (Cambridge Isotope Laboratories) at the MIT Department of Chemistry Instrumentation Facility (DCIF) on either a Mercury 300 or an Inova 500 spectrometer at 25 °C. All chemical shifts are reported in the standard δ notation in parts per million; positive chemical shifts are to higher frequency from the given reference. Absorption spectra were obtained on either a Cary-17 spectrophotometer modified by On-Line Instruments (OLIS) to include computer control or a Spectral Instruments 440 Series spectrophotometer. Differential scanning calorimetry (DSC) was carried out on a Perkin-Elmer Pyris 1 differential scanning calorimeter. Samples were run under a nitrogen atmosphere. Thermal gravimetric analyses with in situ infrared detection were performed on a Perkin-Elmer 3000 TG-IR system. High-resolution mass spectral analyses were carried out at the University of Illinois Mass Spectrometry Laboratory or the MIT Department of Chemistry Instrumentation Facility. Elemental analyses were carried out at Quantitative Technologies, Inc. (Whitehouse, NJ) and Michigan State University.

Hydrogen Peroxide Disproportionation Reactions. Dismutation reactions were performed at room temperature in a 5 mL conical reaction vial with a side port, equipped with a magnetic spinvane stir bar and a capillary gas delivery tube linked to a graduated buret filled with water. The reaction vial was charged with 1 μmol of the iron porphyrin, 25 μmol of 1,5-dicyclohexylimidazole, 4 μmol of benzyldimethyltetradecylammonium chloride, 2 mL of dichloromethane, and 1 mL of phosphate buffer, pH 7. The solution was stirred to ensure gas pressure equilibration. An aliquot of 30% H_2O_2 (0.11 mL) was added to the reaction mixture via syringe through the side port. The oxygen evolution was measured by use of a buret. The identity of the oxygen gas was confirmed independently by the alkaline pyrogallol test.[137]

(137) Duncan, I. A.; Harriman, A.; Porter, G. *Anal. Chem.* **1979**, *51*, 2206–2208.

Olefin Epoxidation Reactions. Epoxidations were carried out at room temperature in air in a 5 mL conical reaction vial equipped with a magnetic spinvane stir bar and a Teflon-lined screw cap. The reaction vial was charged with 1 μmol of the manganese porphyrin, 500 μmol of styrene or *cis*-cyclooctene, 20 μmol of 1,5-dicyclohexylimidazole, 2.75 μmol of *n*-dodecane (standard), and 2 mL of dichloromethane. The solution was stirred, and at regular intervals of 1 h, an aliquot of 0.23 mL of 30% H_2O_2 (2940 μmol, pH adjusted at 4−4.5 with 1% aqueous NaOH) was added to the reaction mixture. The reactions were stopped after 3 h. An aliquot of the reaction mixture was then withdrawn for gas chromatographic (GC) analyses with *n*-dodecane as a standard. Product analyses for the styrene and *cis*-cyclooctene epoxidation reactions were performed on a Hewlett-Packard 5890 series II gas chromatograph with a Hewlett-Packard-1 nonpolar column (30 m). Retention times for the epoxides prepared in our catalytic reactions are identical to those of authentic samples. Epoxidation of *cis*-stilbene was carried out as described by Groves and Stern[99] and Mansuy and co-workers.[101]

Acknowledgment. C.J.C. kindly thanks the National Science Foundation and the MIT/Merck Foundation for predoctoral fellowships. We also thank D. Papoutsakis and J. Madden for their help with the DSC measurements and C.-Y. Yeh and J. T. Groves for helpful discussions. The National Institutes of Health (GM 47274) provided funding for this work.

JA028548O